

Identification of the gallium vacancy–oxygen pair defect in GaN

N. T. Son,¹ C. G. Hemmingsson,¹ T. Paskova,² K. R. Evans,² A. Usui,³ N. Morishita,⁴ T. Ohshima,⁴ J. Isoya,⁵
B. Monemar,^{1,6} and E. Janzén¹

¹*Department of Physics, Chemistry and Biology, Linköping University, SE-581 83 Linköping, Sweden*

²*Kyma Technologies Inc., 8829 Midway West Road, Raleigh, North Carolina 27617, USA*

³*R&D Division, Furukawa Co., Ltd., Tsukuba, Ibaraki 305-0856, Japan*

⁴*Japan Atomic Energy Agency, 1233 Watanuki, Takasaki, Gunma 370-1292, Japan*

⁵*Graduate School of Library, Information and Media Studies, University of Tsukuba, Tsukuba, Ibaraki 305-8550, Japan*

⁶*The Nanometer Structure Consortium, Lund University, P.O. Box 118, S-221 00 Lund, Sweden*

(Received 4 July 2009; revised manuscript received 30 August 2009; published 28 October 2009)

Cation vacancies like V_{Ga} , V_{Al} and their complexes with oxygen are predicted to be abundant in III-nitrides and to play an important role in nonradiative recombination. Appearing in triple or double negatively charged states, they are not paramagnetic and have not so far been detected by magnetic resonance even under illumination. In this Brief Report, we demonstrate an efficient way to make cation vacancy defects in GaN detectable by electron paramagnetic resonance and present our identification of the $V_{\text{Ga}}\text{O}_{\text{N}}$ pair in GaN which is the model material for the III-nitrides and their alloys.

DOI: [10.1103/PhysRevB.80.153202](https://doi.org/10.1103/PhysRevB.80.153202)

PACS number(s): 71.55.Eq, 61.72.jd, 61.82.Fk, 76.30.Mi

Theoretical calculations have predicted low formation energies for the cation vacancy (V_{Ga} , V_{Al}) in n -type GaN and AlN.^{1,2} Later calculations suggested that complexes between the cation vacancy and oxygen have even lower formation energies than the isolated vacancy.³ V_{Ga} and its complexes, such as the $V_{\text{Ga}}\text{O}_{\text{N}}$ pair, are therefore expected to be abundant in as-grown undoped GaN, which is n -type conducting due to the contamination with O and/or Si during the growth. V_{Ga} and its complexes with O, were found to be dominating defects in as-grown GaN by positron annihilation spectroscopy (PAS).^{4,5} From the excitation dependence, the yellow (YL) and green (GL) luminescence bands were assigned to two charge states of a defect presumably the $V_{\text{Ga}}\text{O}_{\text{N}}$ pair.⁶ From a combination of time-resolved photoluminescence, measuring nonradiative recombination times, and PAS studies, detecting cation vacancies and their related complexes, Chichibu *et al.*⁷ found that the nonradiative recombination process in GaN is governed by V_{Ga} -defect complexes. Cation vacancy complexes have recently been suggested to be the major nonradiative defects in InGaN quantum well structures employed for visible light emitters,⁸ and recently AlGaIn structures employed for UV emitters.⁹ The control of cation vacancy defects is therefore important for improving the quantum efficiency of the III-nitride based light emitting devices. The defect identification depends largely on data from magnetic resonance such as electron paramagnetic resonance (EPR) or optical detection of magnetic resonance (ODMR). However, cation vacancy defects in the III-nitrides may capture three more electrons and are in EPR inactive charge states (3- for single vacancies and 2- for vacancy-oxygen pairs with the electron spin $S=0$). They have not so far been detected by EPR or even by ODMR which with optical excitation can change the charge state of defects in many cases. It seems that in the III-nitrides the excited electrons recombine to the original levels so fast that optical excitation alone cannot efficiently activate other charge states of cation vacancy defects. So far, only the double positive Ga interstitial, Ga_i^{2+} , has been identified in irradiated GaN by Chow and

co-workers.^{10–12} In undoped n -type and Mg-doped p -type GaN, a number of defects were observed and assigned to impurities^{13,14} or Mg-Ga interstitial complexes.¹⁵ However, in p -type GaN cation vacancy defects have high formation energies^{1–3} and are expected to have low concentrations. Therefore, p -type materials may be not suitable for the study of cation vacancy defects.

In this Brief Report, we show that using electron irradiation to create high concentrations of electron traps in combination with illumination is an efficient way to make cation vacancy defects in GaN detectable by EPR. The approach is applied for the identification of the $V_{\text{Ga}}\text{O}_{\text{N}}$ pair defect in GaN.

The samples used in the study are n -type nominally undoped and Si-doped bulk GaN grown by hydride vapor phase epitaxy on sapphire substrates. Thick (~ 0.6 – 1.1 mm) free-standing GaN layers were self-separated from the substrates. The undoped samples can be divided into low- and high-doping sets. The residual donor concentration (taken as the average of the concentrations determined by C-V and Hall-effect measurements) is in the range of 1 – 3×10^{16} cm^{-3} for low-doped samples and ~ 5 – 8×10^{17} cm^{-3} for the high-doped samples. The freestanding Si-doped layers are 0.45-mm thick with the Si concentration of $\sim 1 \times 10^{18}$ cm^{-3} . The irradiation with 2-MeV electrons was performed at room temperature with different doses varying from 2×10^{18} to 1×10^{19} cm^{-2} . EPR experiments were performed on an X-band Bruker E580 spectrometer. For illumination, a Xenon lamp, a 0.25-m single grating Jobin-Yvon monochromator and appropriate optical filters were used.

In our as-grown undoped samples, only the EPR spectrum of the shallow donor¹³ was observed. After irradiation, the signal of the shallow donor disappeared. Figure 1(a) shows a broad signal with an isotropic g value ~ 2.03 , labeled D1, observed in a sample irradiated to a dose of 1×10^{19} cm^{-2} . After exposing the sample to weak room light during cooling down, a strong EPR spectrum, labeled D2, was observed [Fig. 1(b)]. In samples irradiated with an electron dose $\sim 6 \times 10^{18}$ cm^{-2} , the D2 signal is weak and the spectrum is

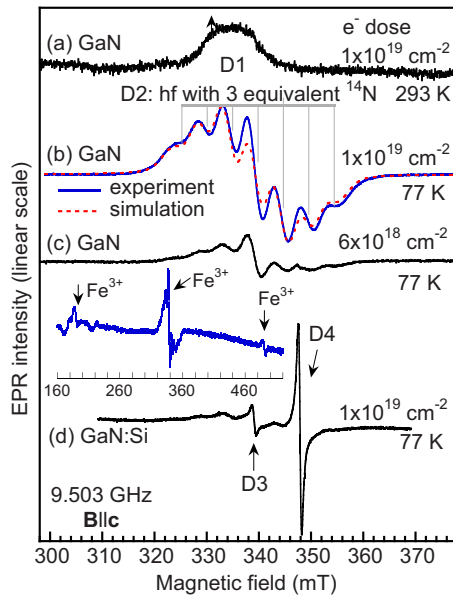


FIG. 1. (Color online) EPR spectra measured for $\mathbf{B}||c$ in n -type GaN irradiated with 2 MeV electrons (a) at 293 K, (b and c) at 77 K, and (d) in Si-doped GaN at 77 K. The electron dose is $6 \times 10^{18} \text{ cm}^{-2}$ for the sample in (c) and $1 \times 10^{19} \text{ cm}^{-2}$ for the samples in (a), (b), and (d). The spectra in (b)–(d) were measured in the same conditions and the intensity is normalized to the sample mass.

dominated by the central line as can be seen in Fig. 1(c). This central line is due to the overlapping of the D2 signal with another line, labeled D3, as will be shown later in annealed or Si-doped samples, and with the signal of the Fe^{3+} center¹⁶ as shown in the inset. The hf structure of D2 consists of seven lines with an equal splitting of ~ 4.7 mT. The structure containing an odd number of hf lines with a central line is typical for nuclei with an integer nuclear spin like ^{14}N . With $I=1$ and 100% natural abundance, the interaction with three equivalent ^{14}N will give rise to seven hf lines with the relative intensity 1, 3, 6, 7, 6, 3, and 1. The simulation of the hf interaction with three equivalent ^{14}N using the hf splitting of 4.7 mT and a line width of 3 mT is plotted in Fig. 1(b) together with the experimental spectrum. The deviation between the simulation and experimental spectra for the central line may be due to the overlapping with the D3 and Fe^{3+} signals. The hf splitting of 4.7 mT is likely due to the interaction with three nearest ^{14}N neighbors of a defect at a Ga site. The D2 defect is therefore likely to be a V_{Ga} -complex (the isolated V_{Ga} would have the hf interaction with four ^{14}N neighbors). The defects that have the hf interaction with three nearest equivalent N neighbors as D2, can be either (i) a pair of V_{Ga} and an impurity with a nuclear spin $I=0$ or (ii) a pair of V_{Ga} with another intrinsic defect such as the $V_{\text{Ga}}V_{\text{N}}$ divacancy with electron spins mainly localized at V_{Ga} and a negligible spin density at V_{N} (the $V_{\text{Ga}}\text{Ga}$ antisite pair can be ruled out since no hf structures of ^{69}Ga and ^{71}Ga could be detected). The best candidate impurity for the former case (i) is oxygen, which occupies the N site and is present in relatively high concentrations even in undoped GaN. The latter case (ii) may be similar to the case of the neutral divacancies

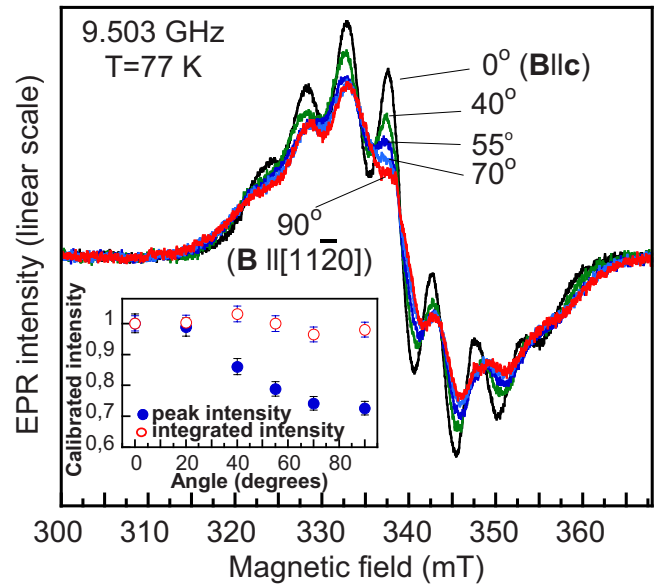


FIG. 2. (Color online) The D2 spectra measured at different directions of \mathbf{B} in the $(1\bar{1}00)$ plane. The inset shows the angular dependence of the integrated intensity of the D2 spectrum and the peak intensity of the central line.

in SiC which show a strong hf interaction with three nearest C neighbors of V_{Si} and negligible hf interactions with nearest Si neighbors of V_{C} .¹⁷ If D2 is related to a pair of intrinsic defects such as the divacancy, its EPR signal is also expected to be dominating in Si-doped samples.

In electron-irradiated (dose $\sim 1 \times 10^{19} \text{ cm}^{-2}$) Si-doped samples, two single line spectra, labeled D3 and D4, were observed [Fig. 1(d)]. Within the experimental error, the D3 spectrum is isotropic ($g=2.0036$). As will be shown later in annealed samples, the D3 signal is present in all irradiated samples. The D4 signal is also detected in several irradiated undoped GaN samples and not specifically related to Si doping. The D4 line is anisotropic with $g_{||}=1.9529$ and $g_{\perp}=1.9505$. The hf structure of D2 was also seen [Fig. 1(d)], but it is very weak compared to the signal in undoped samples [Fig. 1(b)]. The suppression of the D2 signal in the Si-doped sample suggests that the second component of the pair is not an intrinsic defect but an impurity with a nuclear spin $I=0$. Except oxygen, there are no other residual impurities which have a nuclear spin $I=0$ and are abundant in GaN. Thus, the $V_{\text{Ga}}\text{O}_{\text{N}}$ pair appears to be the best model for the D2 defect.

Figure 2 shows EPR spectra in an irradiated GaN sample measured for different directions of the magnetic field \mathbf{B} with respect to the c axis in the $(1\bar{1}00)$ plane (0° corresponds to $\mathbf{B}||c$ and 90° to $\mathbf{B}\perp c$ and $\mathbf{B}||[1\bar{1}20]$). At angles close to the c axis (0° – 20°), the line width as measured from the maximum to minimum of the absorption line is about 2.8 mT and the hf lines are well resolved (Fig. 2). The hf lines get broader (up to ~ 3.8 mT) at angles between 50° and 70° . The angular dependence of the integrated intensity of the D2 spectra and the peak height of the central line are plotted in the inset of Fig. 2, showing the decrease in the peak intensity of the central line and a constant integrated intensity of the

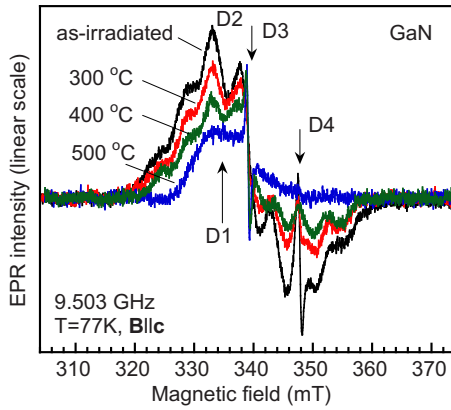


FIG. 3. (Color online) EPR spectra from an electron-irradiated n -type GaN sample measured before and after annealing at different temperatures.

D2 spectrum. This suggests that the line splits when \mathbf{B} is not parallel to the c axis due to a low symmetry C_{1h} of the hf tensor, which is expected for the hf interaction with three N neighbors, and the g tensor (there are C_{1h} defect configurations in addition to the one with C_{3v} symmetry as expected for a close pair defect). From the angular dependence, the electron spin is shown to be $S=1/2$ and the g values for the C_{3v} center are determined as $g_{\parallel}=2.001$ and $g_{\perp}=1.999$. The anisotropy of the hf splitting is about 0.3 mT (~ 4.7 mT for $\mathbf{B} \parallel \mathbf{c}$ and ~ 5.0 mT for angles close to 70°).

An annealing study was performed on the same sample in N_2 gas flow for 10 min at each temperature. In this sample, the D4 signal was already detected before annealing while the D3 signal is merged into the central line of D2. After annealing at 300°C , the D2 and D4 signals start decreasing (the integrated intensity of D2 is reduced by a factor two) and the D3 signal can be clearly seen (Fig. 3). This behavior is similar to that of V_{Ga} -related complexes in GaN irradiated with 2 MeV electrons as studied by PAS (50% reduction after annealing at ~ 600 K).¹⁸ The D2 and D4 spectra were not detected after annealing at 500°C . From the predicted binding energy of ~ 1.8 eV,¹ the $V_{\text{Ga}}\text{O}_N$ pair is expected to be stable at higher temperatures. It is possible that the D2 defect is not annealed out at 500°C but the activation of the negative charge state of the $V_{\text{Ga}}\text{O}_N$ pair by illumination became less effective due to annealing out of higher-lying electron traps.

From the hf structure of three equivalent ^{14}N , the suppression of the signal in Si-doped samples and the spin $S=1/2$, we identify the D2 defect as the $V_{\text{Ga}}\text{O}_N$ pair in the negative charge state. In complete darkness, the Fermi level in irradiated samples may still lie above or at the $(1-|2-)$ level and the pair is in the $2-$ charge state. In heavily irradiated samples (electron doses $\sim 6 \times 10^{18} - 1 \times 10^{19}$ cm^{-2}), the concentration of radiation-induced defects is high. This facilitates the process of removal electrons from the $(1-|2-)$ level to the higher-lying electron traps, turning the defect to the singly negatively charged state $(0|-)$ which has $S=1/2$ and can be detected by EPR. Figure 4(a) shows the D2 spectra observed under illumination with light of different photon energies. Here, the negative charge state has partly been activated due to background light during cooling down and the

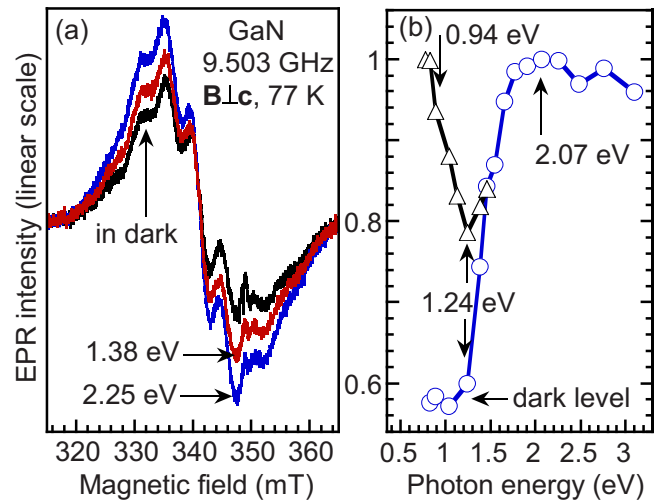


FIG. 4. (Color online) (a) The D2 spectra measured in darkness and under illumination and (b) the dependence of its calibrated intensity on the photon energy. The first data set (\circ) is from the measurements starting when the EPR intensity is minimum (the dark level) whereas the second data set (\triangle) represents measurements repeated after the intensity had reached its maximum.

D2 signal was detected already in darkness [Fig. 4(a)]. The D2 signal starts increasing when the photon energy is $h\nu \sim 1.24$ eV and reaches the maximum at $h\nu \sim 2.1-2.3$ eV [Fig. 4(b)]. We found no noticeable changes in the signal after switching off the light for a day. The photoexcitation induced changes in the EPR intensity can be explained as follows. The illumination with $h\nu \sim 1.24$ eV or higher excited electrons from the $(1-|2-)$ level directly to the higher-lying electron traps and changes the charge state from doubly to singly negative for a part of the total concentration of the $V_{\text{Ga}}\text{O}_N$ pair. At low temperatures, the captured electrons stay at the traps. This explains why the D2 signal can be detected in complete darkness after exposing the sample to light. The direct transitions from the level to higher-lying traps are intercenter transitions and hence less efficient. The removal of electrons from the $(1-|2-)$ level becomes more efficient when electrons can be excited to the conduction band (CB) and then recombine to all available higher-lying traps. Thus, the photon energies $h\nu \sim 2.1-2.3$ eV, corresponding to the maximum EPR intensity, can be interpreted as the energy distance from the $(1-|2-)$ level to CB. This places the $(1-|2-)$ level at $\sim 1.2-1.4$ eV above the valence band maximum, E_V , (with the band gap of ~ 3.49 eV for GaN at 77 K and assuming a negligible Franck-Condon shift). Next, we repeat again photo-EPR measurements with the EPR intensity at its maximum (after illuminating with light of $h\nu \sim 2.25$ eV). As can be seen in Fig. 4(b), the signal starts decreasing when $h\nu \sim 0.94$ eV and continues the trend to a minimum which is not the same as the dark level but $\sim 25\%$ higher. When $h\nu \geq 1.24$ eV the signal starts increasing again and follows the intensity dependence of the previous measurements. We assign the threshold of ~ 0.94 eV to the energy distance from the valence band maximum to the $(0|-)$ level of $V_{\text{Ga}}\text{O}_N$. Thus, the $(0|-)$ and $(1-|2-)$ levels are located at $\sim E_V + 0.94$ eV (or $\sim E_C - 2.55$ eV) and at $\sim E_V + (1.2-1.4)$ eV [or $\sim E_C - (2.1-2.3)$ eV], respectively. The energy for the

(1-|2-) level is slightly higher than the value of 1.1 eV predicted by calculations.¹ The obtained energies of E_C (-2.1–2.3) eV and E_C -2.55 eV correlate very well with the energies of the broad YL (at 2.2 eV) and GL (at 2.5 eV) luminescence bands. Therefore, these luminescence bands can be explained by optical transitions from the conduction band and/or shallow donor levels to the (1-|2-) and (0|-) levels of $V_{\text{Ga}}\text{O}_{\text{N}}$. Our result supports the finding on the involvement of two charge states in the YL and GL bands.⁶

In summary, we have demonstrated that using electron irradiation to create a high concentration of electron traps in combination with illumination is an efficient way to make cation vacancy defects in GaN detectable by EPR. Four EPR defects labeled D1–D4 were observed. Among these, D2 is

the dominating defect in heavily irradiated undoped n -type GaN. Based on the observed hf structure of three ^{14}N neighbors and the suppression of the signal in Si-doped samples, the D2 defect is identified as the negative $V_{\text{Ga}}\text{O}_{\text{N}}$ pair. For the axial defect configuration, the g values are $g_{\parallel}=2.001$ and $g_{\perp}=1.999$. The (1-|2-) and (0|-) levels of the pair are found to be located at $\sim E_V+(1.2-1.4)$ eV and at $\sim E_V+0.94$ eV, respectively. The YL and GL luminescence bands can be explained by the optical transitions from the conduction band and/or shallow donor levels to the (1-|2-) and (0|-) acceptor levels, respectively, of the $V_{\text{Ga}}\text{O}_{\text{N}}$ pair.

Support from the Swedish Foundation for Strategic Research and the Swedish Research Council is acknowledged.

¹J. Neugebauer and C. G. Van de Walle, Appl. Phys. Lett. **69**, 503 (1996).

²C. G. Van de Walle and J. Neugebauer, J. Appl. Phys. **95**, 3851 (2004).

³T. Mattila and R. M. Nieminen, Phys. Rev. B **55**, 9571 (1997).

⁴K. Saarinen *et al.*, Phys. Rev. Lett. **79**, 3030 (1997).

⁵K. Saarinen, T. Suski, I. Grzegory, and D. C. Look, Phys. Rev. B **64**, 233201 (2001).

⁶M. A. Reshchikov, H. Morkoc, S. S. Park, and K. Y. Lee, Appl. Phys. Lett. **81**, 4970 (2002).

⁷S. F. Chichibu, A. Uedono, T. Onuma, T. Sota, B. A. Haskell, S. P. DenBaars, J. S. Speck, and S. Nakamura, Appl. Phys. Lett. **86**, 021914 (2005).

⁸S. F. Chichibu *et al.*, Nature Mater. **5**, 810 (2006).

⁹S. F. Chichibu, A. Uedono, T. Onuma, S. P. DenBaars, U. K. Mishra, J. S. Speck, and S. Nakamura, Mater. Sci. Forum **590**, 233 (2008).

¹⁰K. H. Chow, G. D. Watkins, A. Usui, and M. Mizuta, Phys. Rev. Lett. **85**, 2761 (2000).

¹¹K. H. Chow, L. S. Vlasenko, P. Johannesen, C. Bozdog, G. D. Watkins, A. Usui, H. Sunakawa, C. Sasaoka, and M. Mizuta, Phys. Rev. B **69**, 045207 (2004).

¹²C. Bozdog, G. D. Watkins, H. Sunakawa, N. Kuroda, and A. Usui, Phys. Rev. B **65**, 125207 (2002).

¹³W. E. Carlos, J. A. Freitas, Jr., M. A. Khan, D. T. Olson, and J. N. Kuznia, Phys. Rev. B **48**, 17878 (1993).

¹⁴E. R. Glaser *et al.*, Phys. Rev. B **65**, 085312 (2002) and references therein.

¹⁵G. N. Aliev, S. Zeng, S. J. Bingham, D. Wolverson, J. J. Davies, T. Wang, and P. J. Parbrook, Phys. Rev. B **74**, 235205 (2006).

¹⁶E. Malguth, A. Hoffmann, W. Gehlhoff, O. Gelhausen, M. R. Phillips, and X. Xu, Phys. Rev. B **74**, 165202 (2006).

¹⁷N. T. Son, P. Carlsson, J. ul Hassan, E. Jánzén, T. Umeda, J. Isoya, A. Gali, M. Bockstedte, N. Morishita, T. Ohshima, and H. Itoh, Phys. Rev. Lett. **96**, 055501 (2006).

¹⁸F. Tuomisto, V. Ranki, D. C. Look, and G. C. Farlow, Phys. Rev. B **76**, 165207 (2007).